Image analysis using separable discrete moments of Charlier-Tchebichef

Mhamed Sayyouri, Abdeslam Hmimid and Hassan Qjidaa

Abstract—In this paper, we propose a new set of separable two-dimensional discrete orthogonal moments called Charlier-Tchebichef's moments. This set of moments is based on the bivariate discrete orthogonal polynomials defined from the product of Charlier and Tchebichef discrete orthogonal polynomials with one variable. We also present an approach for fast computation of Charlier-Tchebichef's moments by using the image slice representation. In this approach the image is decomposes into series of non-overlapped binary slices and each slice is described by a number of homogenous rectangular blocks. Once the image is partitioned into slices and blocks, the computation of Charlier-Tchebichef's moments can be accelerated, as the moments can be computed from the blocks of each slice. A novel set of Charlier-Tchebichef invariant moments is also presented. These invariant moments are derived algebraically from the geometric invariant moments and their computation is accelerated using an image representation scheme. The presented approaches are tested in several well known computer vision datasets including computational time, image reconstruction, moment's invariability and classification of objects. The performance of these invariant moments used as pattern features for a pattern classification is compared with Tchebichef-Krawtchouk, Tchebichef-Hahn and Krawtchouk-Hahn invariant moments

Keywords—Charlier-Tchebichef's invariant moments, Image reconstruction, Pattern recognition, Classification.

I. INTRODUCTION

The image moments has been widely used successfully for image analysis and pattern recognition [1-5]. Hu is the first who introduced the geometric moments in pattern recognition [1]. The non orthogonal property of geometric moments causes the redundancy of information. To overcome this problem, the continuous orthogonal moments as Legendre [2], Zernike [2], Gegenbauer [3] and Fourier-Mellin [4] are introduced in the fields of image. The orthogonal property of continuous moments assures the robustness against noise and eliminates the redundancy of information [2-4], but their computation requires the discretization of continuous space and the approximation of the integrals which increases the computational complexity and causes the discretization error [5-9]. To eliminate this error, the discrete orthogonal moments such as Tchebichef [8], Krawtchouk [9] and Hahn [10] have been introduced in image analysis and pattern recognition. The

F. M.Sayyouri, A.Hmimid and H. Qjidaa are with the CED-ST, LESSI, Faculty of sciences Dhar El Mehraz,University Sidi Mohamed Ben Abdellah, BP 1796 Fez-Atlas 30030, Fez, Morocco
E-mail: mhamedsay@yahoo.fr, abdeslam_ph@yahoo.fr , qjidah@yahoo.fr.

use of this set of moments eliminates the need for numerical approximation [11]. All of continuous and discrete orthogonal moments have separable basic functions that can be expressed as two separate terms by producing the two same classical orthogonal polynomials with one variable. Recently, a novel set of discrete and continuous orthogonal moments based on the bivariate orthogonal polynomials have been introduced into the field of image analysis and pattern recognition [12-14]. These series of bivariate polynomials are solutions of the second-order partial differential equations [15-16]. A general method for generating bivariate continuous orthogonal polynomials from continuous orthogonal polynomials with one variable is given by Koornwinder in [17]. Dunkl and Xu in [18] have proposed an excellent paper of bivariate discrete orthogonal polynomials as a product of two families of classical discrete orthogonal polynomials with one variable. Zhu has studied in [12] seven types of continuous and discrete orthogonal moments based on the tensor product of two different orthogonal polynomials with one variable. The computation of discrete orthogonal moments is limited by the high computational cost and the propagation of numerical error in the computation of polynomials values [19]. To limit this error the Scientists apply the recurrence relation with respect to variable x instead of order n in the computation of discrete orthogonal polynomials [19]. To reduce the computational time cost of moments, several algorithms are introduced in literature [20-26]. If the most work has focused on the discrete and continuous moments based on the product of the two same classical orthogonal polynomials with one variable, no attention has been paid to accelerate the time computation of discrete orthogonal moments based on the product of two different discrete orthogonal polynomials with one variable. In this paper, we present a new set of discrete orthogonal moments based on the product of Charlier and Tchebichef discrete orthogonal polynomials which are denoted Charlier-Tchebichef moments (CTM). We also present an approach to accelerate the time computation of CTM based on:

1) The methodology of image slices representation (ISR): In this method the image is decomposes into series of non-overlapped binary slices and each slice is described by a number of homogenous rectangular blocks. Once the image is partitioned into slices and blocks, the computation of CTM can be accelerated, as the moments can be computed from the blocks of each slice.

2) The computation the bivariate discreet orthogonal polynomials of Charlier-Tchebichef by using the recurrence relation with respect to variable x instead of order n.

The paper also tests the ability of CTM for image reconstruction and classification of objects. For the purpose of objects classification, it is vital that presented CTM is independent of rotation, scaling and translation of the image. For this, we have proposed a new set of discrete invariant moments of Charlier-Tchebichef (CTMI) under translation, scaling and rotation of the image. The CTMI is derived algebraically from the geometric invariant moments. A fast computation algorithm of CTMI is also presented using the image slice representation methodology (ISR). The accuracy of object classification by our descriptors CTMI is compared with Tchebichef-Krawtchouk invariant moments (TKMI) [12], Tchebichef-Hahn invariant moments (THMI) [12] and Krawtchouk-Hahn (KHM)[12] invariant moments. The rest of the paper is organized as follows: In Section 2, we present the known results of the Charlier and Tchebichef discrete orthogonal polynomials with one variable and the bivariate discrete orthogonal polynomials of Charlier -Tchebichef. Section 3 studies the computation of CTM discrete moments by two methods: the direct method and the fast method. The image reconstruction by CTM is given in section 4. Section 5 focuses on the deriving of CTMI from the geometric moments by two methods. Section 6 provides some experimental results concerning the time computation of CTM, image reconstruction by CTM and the invariability and objects classification by CTMI. Section 7 concludes the work.

II. CLASSICAL DISCRETE ORTHOGONAL POLYNOMIALS

In this section, we will present a brief introduction to the theoretical background of discrete orthogonal polynomials with one variable of Tchebichef and Charlier [29-30].

A. Tchebichef's polynomials

The discrete orthogonal polynomials of Tchebichef with one variable $t_n(\text{x};\text{N-1})$ satisfy the following first-order partial difference equation [30]:

$$(N - x)x\Delta\nabla t_n(x;N-1) + (N-1-2x)\Delta t_n(x;N-1)$$
$$+ n(n+1)t_n(x;N-1) = 0 \qquad (1)$$

with   x , n $= 0, 1, 2….N-1$

The operators $\Delta t_n(x;N-1) = t_n(x+1;N-1) - t_n(x;N-1)$ and $\nabla t_n(x;N-1) = t_n(x;N-1) - t_n(x-1;N-1)$ denote the forward and backward finite difference operators, respectively.

The nth Tchebichef polynomial is defined by using hypergeometric function as:

$$t_n(x;N-1) = (1-N)_n\,_3F_2(-n,-x,1+n;1,1-N;1)$$
$$= \sum_{i=0}^{n} \delta_{m,i}x^i \qquad (2)$$

where $_3F_2$ is the generalized hypergeometric function given

by:

$$_3F_2(a_1,a_2,a_3;b_1,b_2;z) = \sum_{k=0}^{\infty} \frac{(a_1)_k(a_2)_k(a_3)_k}{(b_1)_k(b_2)_k}\frac{z^k}{k!} \qquad (3)$$

The normalized discrete orthogonal polynomials of Tchebichef are defined by:

$$\tilde{t}_n(x;N-1) = t_n(x;N-1)\sqrt{\frac{1}{\rho_t(n)}} \qquad (4)$$

with $\rho_t(n)$ is the squared norm of Tchebichef polynomials defined as:

$$\rho_t(n) = \frac{(N+n)!}{(2n+1)(N-n-1)!} \qquad (5)$$

Such that the orthogonal condition is defined as:

$$\sum_{x=0}^{N} \tilde{t}_n(x;N)\tilde{t}_m(x;N) = \delta_{nm} \qquad (6)$$

where δ_{nm} denotes the Dirac function.

To compute the discrete orthogonal polynomials of Tchebichef, we use the recurrence relation with respect to variable x.

By considering the properties of the operators Δ and ∇ we have:

$$\Delta\nabla t_n(x;N-1) = t_n(x+1;N-1) - 2t_n(x;N-1) + t_n(x-1;N-1) \qquad (7)$$

Thus, the recurrence relations of Tchebichef discrete orthogonal polynomials with respect to variable x can be obtained through (1) and (7) as follows:

$$t_n(x;N-1) = \frac{2(x-1)(N-x+1) + (N-2x+1) - n(n+1)}{(x-1)(N-x+1) + (N-2x+1)}t_n(x-1;N-1)$$
$$- \frac{(x-1)(N-x+1)}{(x-1)(N-x+1) + (N-2x+1)}t_n(x-2;N-1) \qquad (8)$$

The initial values of recurrence relation with respect to variable x are defined as:

$$t_n(0;N-1) = (-1)^n(N-n)_n,$$
$$t_n(1;N-1) = (1 + \frac{n(n+1)}{1-N})t_n(0;N-1) \qquad (9)$$

B. Charlier's polynomials

The discrete orthogonal polynomials of Charlier $C_n^{a_1}(x)$ satisfy the following first-order partial difference equation [29-30].

$$x\Delta\nabla C_n^{a_1}(x) + (a_1 - x)\Delta C_n^{a_1}(x) + nC_n^{a_1}(x) = 0 \qquad (10)$$

The nth discrete orthogonal polynomials of Charlier $C_n^{a_1}(x)$ are defined by using hypergeometric function as [35]:

$$C_n^{a_1}(x) = {}_2F_0(-n,-x;;1/a_1) = \sum_{k=0}^n \alpha_{k,n}^{(a_1)} x^k \tag{11}$$

where $x = 0,1,2\ldots$; $n \geq 0$; $a_1 > 0$

${}_2F_0$ is the hypergeometric function defined as:

$$_2F_0(a,b;-;x) = \sum_{k=0}^{\infty} (a)_k (b)_k \frac{x^k}{k!} \tag{12}$$

The set of discrete orthogonal polynomials of Charlier $\{C_n^{a_1}(x)\}$ forms a complete set of discrete basis functions with weight function

$$w_c(x) = \frac{e^{-a_1} a_1^x}{x!} \tag{13}$$

and satisfies the orthogonal condition

$$\sum_{x=0}^N w_c(x) C_n^{a_1}(x) C_m^{a_1}(x) = \rho_c(n)\delta_{nm} \tag{14}$$

where $\rho(n)$ is the squared norm of Charlier discrete orthogonal polynomials defined as:

$$\rho_c(\mathrm{n}) = \frac{n!}{a_1^n} \tag{15}$$

To avoid fluctuations in the numerical calculation of Charlier orthogonal polynomial we use their normalized form defined as:

$$\tilde{C}_n^{a_1}(x) = C_n^{a_1}(x)\sqrt{\frac{w_c(x)}{\rho_c(n)}} \tag{16}$$

The recurrence relations of Charlier's discrete orthogonal polynomials with respect to variable x can be obtained through Eq.(7) and Eq.(10) as follows:

$$C_n^{a_1}(x) = \frac{x + a_1 - n - 1}{a_1} C_n^{a_1}(x-1) - \frac{x-1}{a_1} C_n^{a_1}(x-2) \tag{17}$$

The initial values of recurrence relation with respect to variable x are defined as:

$$C_n^{a_1}(0) = 1 \quad \text{and} \quad C_m^{a_1}(1) = \frac{a_1 - n}{a_1} \tag{18}$$

C. Product Charlier-Tchebichef polynomials

The bivariate discrete orthogonal polynomials of Charlier-Tchebichef are obtained from the product of discrete orthogonal polynomials with one variable of Charlier $C_n^{a_1}(x)$ and Tchebichef $t_n(x, N-1)$ [31-33]:

$$Ct_{n,m}(x,y) = C_n^{a_1}(x)t_m(y,N-1) \quad ; n \geq 0 \quad ; 0 \leq m \leq N-1 \tag{19}$$

and are orthogonal on the set $V = \{(i,j): i \in \mathbb{N}_0, \ 0 \leq j \leq N-1\}$ with respect to the weight function of the Charlier-Tchebichef's discrete orthogonal polynomials is defined as:

$$w_{c,t}(x,y) = \frac{(a_1)_x}{x!} \tag{20}$$

III. CHARLIER-TCHEBICHEF MOMENTS

The two-dimensional (2-D) Charlier-Tchebichef's discrete orthogonal moments (CTM) of order (n+m)th of an image intensity function $f(x,y)$ with size MxN is defined as

$$CTM_{nm} = \sum_{x=0}^{M-1}\sum_{y=O}^{N-1} Ct_{n,m}(x,y,N-1)f(x,y)$$
$$= \sum_{x=0}^{M-1}\sum_{y=O}^{N-1} \tilde{C}_n^{a_1}(x)\tilde{t}_n(y,N-1)f(x,y) \tag{21}$$

with $\tilde{C}_n^{a_1}(x)$ and $\tilde{t}_n(y,N-1)$ is the nth order of orthonormal polynomials of Charlier and Tchebichef respectively.

The computation of Charlier- Tchebichef moments by using Eq. (21) seems to be a time consuming task mainly due to the need of computation a set of complicated quantities for each moment order and the need to evaluate the polynomial values for each pixel of the image. To accelerate the computation of Charlier-Tchebichef's moments we will use the methodology of the image slice representation (ISR) [20-21] described as follows.

A. Fast computation of Charlier-Tchebichef moments

In this approach, the image is decomposes into series of binary slices and each slice is represented by a set of blocks, each block corresponding to an object. These blocks are defined as a rectangular area that includes a set of connected pixels. By applying the ISR approach, the image is described by the relation:

$$f(x,y) = \sum_{i=1}^L f_i(x,y) \tag{22}$$

where L is the number of slices and f_i is the intensity function of the ith slice. In the case of a binary image L is 1 and thus $f(x,y) = f_1(x,y)$.

After the decomposition of the image into several slices of two levels, we can apply the algorithm IBR [20]. The image $f(x,y)$ can be redefined in terms of blocks of different intensities

$$f(x,y) = \{f_i(x,y), i = 1,2,\ldots,L\}$$
$$= \{b_{ij}, j = 1,2,\ldots,K_i-1\} \tag{23}$$

where b_{ij} is the block of the edge i and K_i is the number of image blocks with intensity. Each block is described by the coordinates of the upper left and down right corner in vertical and horizontal axes.

The Eq. (19) can be rewritten as:

$$CTM_{nm} = \sum_{x=0}^{N-1}\sum_{y=O}^{N-1}\tilde{C}_n^{a_1}(x)\sum_{i=1}^{L}f_i(x,y)$$

$$= \sum_{i=1}^{L}\sum_{x=0}^{N-1}\sum_{y=O}^{N-1}\tilde{C}_n^{a_1}(x)\tilde{t}_m(y)f_i(x,y)$$

$$= \sum_{i=1}^{L}f_i CTM_{nm}^{b_i} \tag{24}$$

where $CTM_{nm}^{b_i}$ are the (n+m) order Charlier-Tchebichef moments of the ith binary slice.

$$CTM_{nm}^{b_i} = \sum_{x=x_{1,b_i}}^{x_{2,b_i}}\sum_{y=y_{1,b_i}}^{y_{1,b_i}}\tilde{C}_n^{a_1}(x)\tilde{t}_m(y)$$

$$= \sum_{x=x_{1,b_i}}^{x_{2,b_i}}\tilde{C}_n^{a_1}(x)\sum_{y=y_{1,b_i}}^{y_{2,b_i}}\tilde{t}_m(y)$$

$$= S_n(x_{1,b_i},x_{2,b_i})S_m(y_{1,b_i},y_{2,b_i}) \tag{25}$$

with (x_{1,b_i},x_{2,b_i}) and (y_{1,b_i},y_{2,b_i}) are respectively the coordinates in the upper left and lower right block b_i and

$$S_n(x_{1,b_i},x_{2,b_i}) = \sum_{x=x_{1,b_i}}^{x_{2,b_i}}\tilde{C}_n^{a_1}(x) \quad \text{and} \quad S_m(y_{1,b_i},y_{2,b_i}) = \sum_{y=y_{1,b_i}}^{y_{2,b_i}}\tilde{t}_m(y) \tag{23}$$

IV. IMAGES RECONSTRUCTION VIA CHARLIER-TCHEBICHEF MOMENTS

In this section, the image representation capability of Charlier-Tchebichef's moments is shown. The Charlier-Tchebichef's moments of the image are first calculated and subsequently its image representation power is verified by reconstructing the image from the moments.

By solving the equation Eq. (21) and the equation of orthogonality, the image intensity function $f(x,y)$ can be written completely in terms of the Charlier-Tchebichef's moments as:

$$f(x,y) = \sum_{n=0}^{N-1}\sum_{m=0}^{N-1}CTM_{nm}\tilde{C}_n^{a_1}(x)\tilde{t}_m(y) \tag{28}$$

The image intensity function can be represented as a series of Charlier-Tchebichef's polynomials by the Charlier-Tchebichef's moments. If the moments are limited to order max , the series is truncated to

$$\hat{f}(x,y) = \sum_{n=0}^{max}\sum_{m=0}^{n}CTM_{n-m,m}\tilde{C}_n^{a_1}(x)\tilde{t}_m(y) \tag{29}$$

To accelerate the reconstruction processes, we can reconstruct the whole image by a finite number of Charlier-Tchebichef's moments can be accomplished by reconstructing only a small portion the pixels (the upper left and down right pixels are always reconstructed) of each block in each slice. The remaining pixels are assigned intensity equal to the mean value of the intensities of the two reconstructed pixels.

The equation for the pixel reconstruction of each block takes the following form

$$\hat{f}(x_{1,b_j},y_{1,b_j}) = \sum_{n=0}^{M-1}\sum_{m=0}^{N-1}CTM_{n,m}\tilde{C}_n^{a_1}(x_{1,b_j})\tilde{t}_m(y_{1,b_j}) \tag{30}$$

An objective measure based on means squared error (MSE)

is used to characterize the error between the original image $f(x,y)$ and the reconstructed image $\hat{f}(x,y)$:

$$MSE = \frac{1}{MN}\sum_{i=1}^{M}\sum_{j=1}^{N}(f(x_i,y_j)-\hat{f}(x_i,y_j))^2 \tag{31}$$

V. CHARLIER-TCHEBICHEF'S INVARIANT MOMENTS

Given a digital image $f(x,y)$ with size M×N, the geometric moments GM_{nm} are defined using discrete sum approximation as:

$$GM_{nm} = \sum_{x=0}^{N-1}\sum_{y=0}^{N-1}x^n y^m f(x,y) \tag{32}$$

The set of geometric invariant moments (GMI) by rotation, scaling and translation can be written as [1]:

$$GMI_{nm} = GM_{00}^{-\gamma}\sum_{x=0}^{N-1}\sum_{y=0}^{N-1}[(x-\bar{x})\cos\theta + (y-\bar{y})\sin\theta]^n[(y-\bar{y})\cos\theta - (x-\bar{x})\sin\theta]^m \tag{33}$$

with

$$\bar{x} = \frac{MG_{10}}{MG_{00}} \quad ; \quad \bar{y} = \frac{MG_{01}}{MG_{00}} \quad ;$$

$$\gamma = \frac{n+m}{2}+1 \quad ; \quad \theta = \frac{1}{2}\tan^{-1}\frac{2\mu_{11}}{\mu_{20}-\mu_{02}} \tag{34}$$

The (n+m)th central geometric moments is defined in [1] by:

$$\mu_{nm} = \sum_{x=0}^{N-1}\sum_{y=0}^{N-1}(x-\bar{x})^n(y-\bar{y})^m f(x,y) \tag{35}$$

A. Computation of Charlier-Tchebichef 's invariant moments

To use the Charlier-Tchebichef's moments for the objects classification, it is indispensable that be invariant under rotation, scaling, and translation of the image. Therefore to obtain the translation, scale and rotation invariants moments of Charlier-Tchebichef (CTMI), we adopt the same strategy used by Author et al. for Hahn's moments in [26]. That is, we derive the CTMI through the geometric moments using the direct method and the fast method based on image slice representation methodology.

The Charlier-Tchebichef moments of $f(x,y)$ can be written in terms of geometric moments as:

$$CTM_{nm} = [\rho_c(n)\rho_t(m)]^{-1/2}\sum_{x=0}^{M-1}\sum_{y=0}^{N-1}c_n^a(x)t_m(y)f(x,y)$$

$$= [\rho_c(n)\rho_h(m)]^{-1/2}\sum_{i=0}^{n}\sum_{j=0}^{m}\alpha_{n,i}^{(a_1)}\delta_{m,j}GM_{ij} \tag{36}$$

where the nth order of Charlier and Tchebichef discrete orthogonal polynomials are given by:

$$c_n^{a_1}(x) = \sum_{i=0}^{n}\alpha_{n,i}^{(a_1)}x^i \quad \text{and} \quad t_n(y) = \sum_{i=0}^{n}\delta_{m,j}y^i \tag{37}$$

The Charlier-Tchebichef's invariant moments (CTMI)

can be expanded in terms of GMI Eq. (33) as follows:

$$CTMI_{nm} = \sum_{i=0}^{n}\sum_{j=0}^{m}\alpha_{n,i}^{(a_1)}\delta_{m,j}V_{i,j} \tag{38}$$

where $\alpha_{n,i}^{(a_1)}$ and $\delta_{m,j}$ are the coefficients relative to Eq.(37) and $V_{i,j}$ are the parameters defined as:

$$V_{nm} = \sum_{p=0}^{n}\sum_{q=0}^{m}\binom{n}{p}\binom{m}{q}\left(\frac{N \times M}{2}\right)^{((p+q)/2)+1}\left(\frac{N}{2}\right)^{n-p}\left(\frac{M}{2}\right)^{m-p}GMI_{pq} \tag{39}$$

B. Fast computation of Charlier-Tchebichef's invariant moments

In order to accelerate the time computation of CTMI, we will apply the algorithms of image slice representation described previously.

By using the binomial theorem, the GMI defined in Eq.(32) can be calculated as follows:

$$GMI_{nm} = GM_{00}^{-\gamma}\sum_{i=0}^{n}\sum_{j=0}^{m}\binom{n}{i}\binom{m}{j}(\cos\theta)^{i+j}(\sin\theta)^{n+m-i-j}\times(-1)^{m-j}\mu_{m+i-j,n+j-i}$$

$$= \sum_{i=0}^{n}\sum_{j=0}^{m}\binom{n}{i}\binom{m}{j}(\cos\theta)^{i+j}(\sin\theta)^{n+m-i-j}\times(-1)^{m-j}\eta_{m+i-j,n+j-i} \tag{40}$$

where

$$\eta_{nm} = \frac{\mu_{nm}}{GM_{00}^{\gamma}} \tag{41}$$

By applying the IBR algorithm, the normalized central moment defined in Eq. (35) can be calculated as follows:

$$\eta_{nm} = \frac{\mu_{nm}}{GM_{00}^{\gamma}} = \frac{1}{GM_{00}^{\gamma}}\sum_{x=0}^{N-1}\sum_{y=0}^{M-1}(x-\overline{x})^{n}(y-\overline{y})^{m}f(x,y)$$

$$= \frac{1}{GM_{00}^{\gamma}}\sum_{x=0}^{N-1}\sum_{y=0}^{M-1}(x-\overline{x})^{n}(y-\overline{y})^{m}(\sum_{k=1}^{S}f_k(x,y))$$

$$= \frac{1}{GM_{00}^{\gamma}}\sum_{k=1}^{S}f_k\times\sum_{x=0}^{N-1}\sum_{y=0}^{M-1}(x-\overline{x})^{n}(y-\overline{y})^{m}$$

$$= \frac{1}{GM_{00}^{\gamma}}\sum_{k=1}^{S}f_k\times\sum_{j=0}^{k}\left[\left(\sum_{x_k=x_{1,b_j}}^{x_{2,b_j}}(x-\overline{x})^{n}\right)\left(\sum_{y_k=y_{1,b_j}}^{y_{2,b_j}}(y-\overline{y})^{m}\right)\right]$$

$$= \frac{1}{GM_{00}^{\gamma}}\sum_{k=1}^{S}f_k\times\eta_{nm}^{k} \tag{42}$$

where

$$\eta_{nm}^{k} = \sum_{j=0}^{k}\left[\left(\sum_{x_k=x_{1,b_j}}^{x_{2,b_j}}(x-\overline{x})^{n}\right)\left(\sum_{y_k=y_{1,b_j}}^{y_{2,b_j}}(y-\overline{y})^{m}\right)\right] \tag{43}$$

and f_k ; $k=1,2,.....S$ is the slices intensity functions, S is the number of slices in image f . b_j ; $j=1,2,....k$ is the block in each slice. (x_{1,b_i}, y_{1,b_i}) and (x_{2,b_i}, y_{2,b_i}) are respectively the coordinates in the upper left and lower right block b_j .

Using the previous equations Eq. (43) and Eq. (41), the GMI of Eq. (40) can be rewritten as:

$$GMI_{nm} = \sum_{i=0}^{n}\sum_{j=0}^{m}\binom{n}{i}\binom{m}{j}(\cos\theta)^{i+j}(\sin\theta)^{n+m-i-j}\times(-1)^{m-j}\eta_{m+i-j,n+j-i}$$

$$= \frac{1}{GM_{00}^{\gamma}}\sum_{i=0}^{n}\sum_{j=0}^{m}\binom{n}{i}\binom{m}{j}(\cos\theta)^{i+j}(\sin\theta)^{n+m-i-j}\times(-1)^{m-j}\sum_{k=1}^{S}f_k\times\eta_{m+i-j,n+j-i}^{k}$$

$$= \frac{1}{GM_{00}^{\gamma}}\sum_{k=1}^{S}f_k\sum_{i=0}^{n}\sum_{j=0}^{m}\binom{n}{i}\binom{m}{j}(\cos\theta)^{i+j}(\sin\theta)^{n+m-i-j}\times(-1)^{m-j}\times\eta_{m+i-j,n+j-i}^{k} \tag{44}$$

Therefore the CTMI under translation, scaling and rotation of the image can be obtained from the equations Eq. (39), Eq. (44) and the Eq. (36).

VI. RESULTS AND SIMULATIONS

In this section, we give experimental results to validate the theoretical results developed in the previous sections. This section is divided into four sub-sections. In the first sub-section, we will compare the time computation of CTM by the direct method and the proposed method for binary and gray-scale images. In the second one, we will test the ability of CTM for the reconstruction of binary and gray-scale images. In sub-section three, the invariability of CTM under the three transformations translation, scaling and rotation is shown. In the last sub-section, the recognition accuracy of CTMI is tested and compared to other descriptions given in [12] for objects classification.

A. Computational time of CTM

In this sub-section, we will compare the computational time of CTM by two methods: the direct method based on Eq. (21) and the proposed fast method based on the application of image slice representation methodology defined previously by Eq. (24) .The execution-time improvement ratio (ETIR) is used as a criterion [38]. This ratio is defined as ETIR%=(1−Time1/Time2)×100, where Time1 and Time2 are the execution time of the first and the second methods. ETIR=0 if both execution times are identical. Note that, all our numerical experiments are performed in Matlab8 on a PC Dual Core 2.10 GHz, 2GB of RAM.

In the first example, a set of five binary images with size 256×256 pixels (Fig.1) selected from the well-known MPEG-7 CE-shape-1 Part B database [36] were used as test images. The number of blocks (NB) of these images is NB = 608 for Horse, NB = 726 for Crown, NB = 510 for Bird, NB = 446 for Bell, and NB = 283 for Tree. Note that the computation time for the extraction of blocks of each image is approximately 0.1ms. The computational processes are performed 20 times for the moments of Charlier-Tchebichef for each of the five images where the average times of CTM and execution-time improvement ratio (ETIR) are included in Table 1. The obtained results are represented and displayed in Table 1. The result indicates again that the proposed method has a better performance than the direct method in terms of computation time of CTM.

In the second example, a set of five gray-scale images with a size of 128x128 pixels shown in Fig. 2 were used. The number

of slices (NS) and the number of blocks (NB) of these images are (NS=250, NB = 14108) for Lena, (NS=245, NB = 13551) for Plane, (NS=235, NB = 10335) for Mountain, (NS=225, NB = 14086) for Flower and (NS=236, NB = 14384) for Highway and the computation time to extract the blocks of each image are approximately in 1ms. The computational processes are performed 20 times of Charlier-Tchebichef's moments for each of the five images where the average times of CTM and execution-time improvement ratio (ETIR) are included in Table 1. The result indicates also that the proposed fast method has a better performance than the direct method because the computation of CTM by the proposed method depends only on the number of blocks than the image's size.

For both types of images, the computation time of CTM has accelerated considerably and the gain of time arrives until 86% for binary images and 79% for images in grayscale.

Fig.1. Set of test binary images: Horse, Crown, Bird, Bell and Tree.

Fig 2: Gray-scale images: Lena, Plane, Mountain, Flower and Highway.

Table 2: Average times in seconds and reduction percentage of binary and gray-scale images.

	Computational time of CMT for	
	Binary images	Gray-scale images
Direct method	2,66	8,54
Proposed method	0,37	1,72
ETIR %	86,05 %	79,89%

B. Image reconstruction via CTM

In this section, we will discuss the ability of CTM for the reconstruction of the binary and gray-scale images using the two methods: the direct method and the proposed method. To evaluate the capacity of image reconstruction, we will calculate the means squared error (MSE) defined by Eq. (31) between the original and the reconstructed images.

Two numerical experiments have been carried out to verify the image reconstruction capability of the proposed method and the direct method when they are used for binary and gray-scale images. The test of both binary image "Horse": image of size 200x200 (Fig. 3) and the gray-scale image "Lena" of size 256×256 (Fig. 3) is used with a maximum moment order ranging from 0 to 200. Fig. 4 and Fig. 5 show the MSE of the proposed method and the direct method for the binary and the gray-scale images. It is obvious that the MSE decreases as the moment of order increases where the MSE gets near to zero

with increasing time order. When the maximum moments order gets to a certain value, the reconstructed images will be very close to the original ones. The figures also show that the proposed method is efficient in terms of quality of the reconstruction of binary and gray-scale images and faster than the direct method.

Finally we will compare the reconstruction ability of CTM for gray-scale image "Lena" by other set of separable discrete moment's defined in [12], Tchebichef-Krawtchouk moments (TKM), Tchebichef-Hahn moments (THM) and Krawtchouk-Hahn moments (KHM). Fig. 6 shows the MSE of CTM by the proposed method compared to TKM, THM and KHM. From this comparison, the proposed CTM moments is still better compared to that of other moments.

C. Invariability

In this section we test the invariability of Charlier-Tchebichef invariant moments under translation, scale and rotation of the image. For this we will use a gray-scale image "Cat" (Fig.3) whose size is 128x128 pixels chosen from the well-known Columbia database [37]. This image is scaled by a factor varying from 0.5 to 1.5 with interval 0.05, rotated from 00 to 3600 with interval 100 and translated by a vectors varying from (-5,-5) to (5,5). Each translation vector consists of two elements which represent a vertical and a horizontal image shift respectively. All invariant moments of CTMI is calculated up to order two for each transformation. Finally, in order to measure the ability of the CTMI to remain unchanged under different image transformations, we define the relative error between the two sets of invariant moments corresponding to the original image $f(x, y)$ and the transformed image $g(x, y)$ as:

$$E_{CM}(f, g) = \frac{\|CTMI(f) - CTMI(g)\|}{\|CTMI(f)\|}$$

(45)

where $\|\,\|$ denotes the Euclidean norm and $CTMI(f)$; $CTMI(g)$ are invariant moments of Charlier-Tchebichef for the original image f and the transformed image g.

(a)   (b)

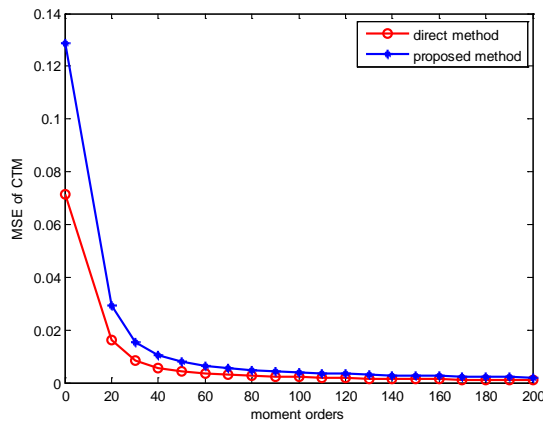Fig. 3. (a) Lena gray-scale image, (b) Horse binary image

Fig. 4. Reconstruction error MSE of CTM for binary image "Horse" by the direct method and the fast method.
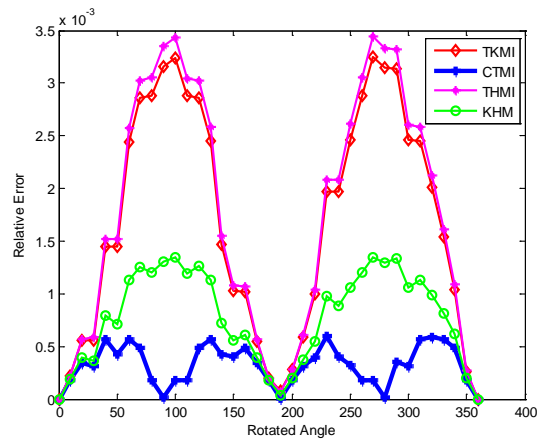

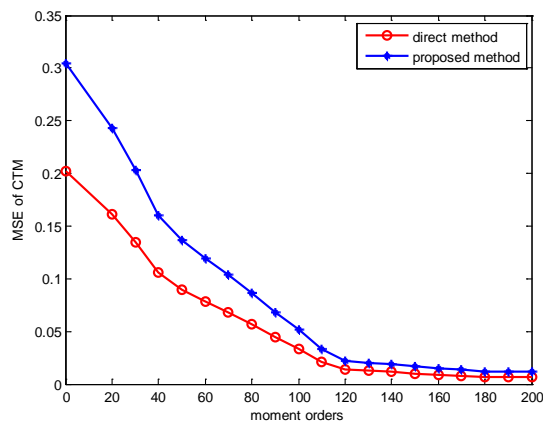Fig. 5. Reconstruction error MSE of CTM for binary image "Horse" by the direct method and the fast method.

Fig. 6. Comparative study of reconstruction error MSE of CTM, TKM, THM and KHM for gray-scale image "Lena" by the fast method.

Fig. 7. Cat gray-scale image

Fig. 8 Comparative study of relative error between the rotated image and the original image by CTMI, TKMI,THMI and KHMI.
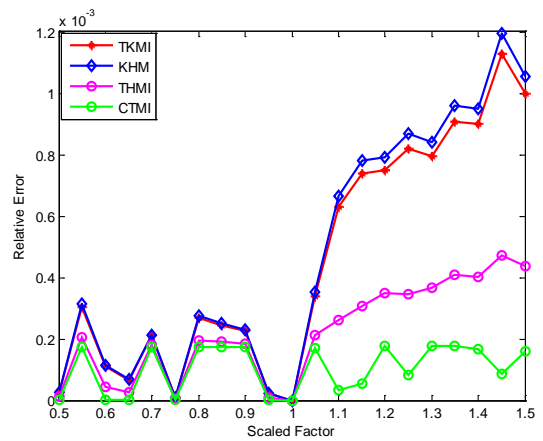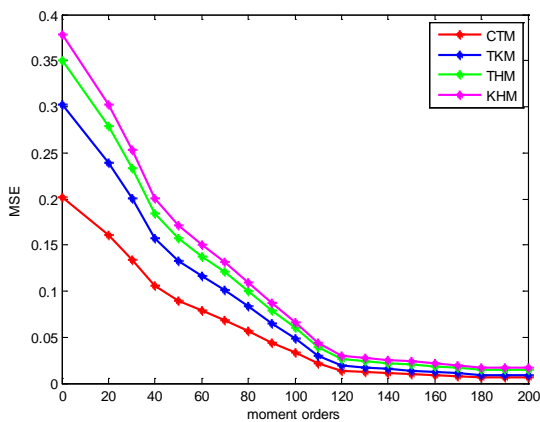

Fig. 9 Comparative study of relative error between the scaled image and the original image by CTMI, TKMI, THMI and KHMI.
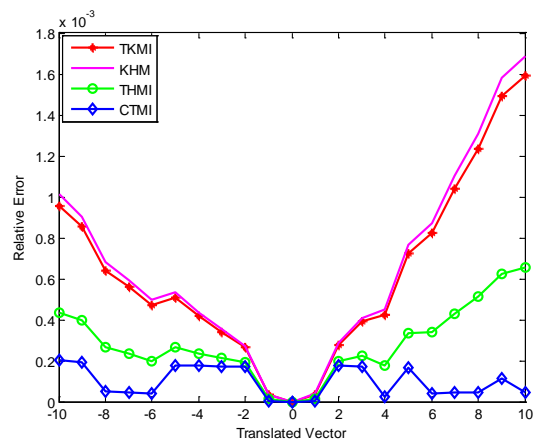

Fig. 10 Comparative study of relative error between the translated image and the original image by CTMI, TKMI, THMI and KHMI.

Fig. 8 compares the relative error between the proposed invariant moments of CTMI, the invariant moments of Tchebichef -Krawtchouk TKMI [12], the invariant of Tchebichef-Hahn THMI [12], and the invariant of Hahn Krawtchouk-HKMI [12], relative to rotation of the image. It can be seen from this figure that the CTMI is more stable

under rotation (very low relative error) and is better performance than the TKMI, THMI and KHMI, whatever the rotational angle.

   Fig. 9 shows the relative error between the CTMI, TKMI, THMI and KHMI relative to scale. The figure shows that, in most cases, the relative error of CTMI is more stable and lower than the TKMI, THMI and KHMI.

   Fig. 10 shows the relative error between the CTMI, TKMI, THMI and KHMI relative to translation. The figure shows again that, in most cases, the relative error of CTMI is more stable and better performance than the TKMI, THMI and KHMI, whatever the translation vectors. Note that, the results are plotted in Figures (7, 8 and 9) for the case $a_1 = 80$ for the Charlier's polynomials, $p = 0.5$ for Krawtchouk's polynomials and $a = b = 10$ for Hahn's polynomials.

The results show that the CTMI is more s table under translation, scale and rotation of the image than the TKMI, THMI and KHMI.

   To test the robustness to noise, we have respectively added a white Gaussian noise (with mean $\mu = 0$ and different variances) and salt-and-pepper noise (with different noise densities). Results are respectively depicted in Figs.10 and 11. It can be seen that, if the relative error increases with the noise level, the proposed descriptors of CTMI are more robust to noise than TKMI, THMI and KHMI.
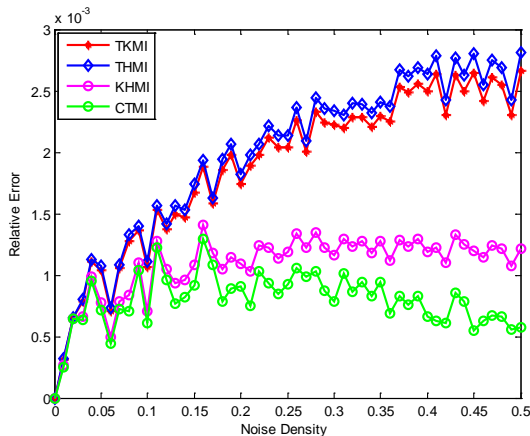

Fig. 11 Comparative study of relative error between the corrupted image (salt & pepper) and the original image by CTMI, TKMI, THMI and KHMI.
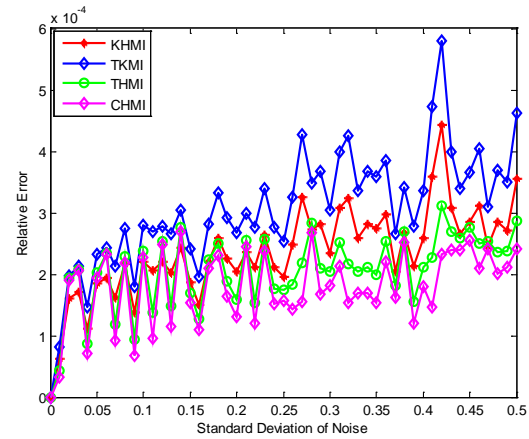

Fig. 12 Comparative study of relative error between the corrupted image (white Gaussian) and the original image by CTMI, TKMI, THMI and KHMI.

D. Classification

   In this section, we will provide experiments to validate the precision of recognition and the classification of objects using the CTMI. For this, we will put in place the characteristic vectors defined by:

$$V = \begin{bmatrix} CTM_{ij} \end{bmatrix} \; ; i, j = 0,1,2 \tag{46}$$

   To perform the classification of the objects to their appropriate classes we will use simple classifiers based on Euclidean distances [35].

$$d(x_s, x_t^{(k)}) = \sqrt{\sum_{j=1}^{n} (x_{sj} - x_{tj}^{(k)})^2} \tag{47}$$

   The above formula measure the distance between two vectors where x_s is the n-dimensional feature vector of unknown sample, and $x_t^{(k)}$ the training vector of class k. If the two vectors x and y are equals, then $d(x, y)$ tend to 0. Therefore to classify the images, one takes the minimum values of the distance.

We define the recognition accuracy as:

$$\eta = \frac{\text{Number of correctly classified images}}{\text{The total of images used in the test}} \times 100\% \tag{48}$$

   In order, to validate the precision of recognition and the classification of objects using the CTMI, we well use two image databases. These bases are standard bases used by the scientific community during the testing and validation of their approach and are freely available on the Internet. Each image database has defined the classes where each image belongs to one class. The first database is MPEG-7 CE-shape-1 Part [36]. This database contains 20 different binary images for 72 objects. Each image is resized in 128x128. This base has the characteristic of being widely used in image classification. The second image database is the Columbia Object Image Library (COIL-20) database [37]. The total number of images is 1440 distributed as 72 images for each object. All images of this database have the size 128x128. We tested the ability of

classification of our descriptor CTMI compared to other descriptors of Tchebichef-Krawtchouk invariant moments (TKMI) [12], Tchebichef-Hahn invariant moments (THMI) [12] and Krawtchouk-Hahn invariant moments (KHMI) [12] for the two databases. The test is followed by adding different densities of salt-and-pepper noise.

The results show the efficiency of the CTMI in terms of recognition accuracy of noisy images, compared to those of THMI, TKMI and KHMI. The comparison results shows the superiority of the proposed moments based on polynomials the Charlier and Tchebichef relative to moments based on the other polynomials. Note that the recognition of non-noisy binary image by our method is 100%, and the accuracy of the recognition decreases with increasing noise.

Finally, the proposed CTMI are robust to image transformations under noisy conditions, and the recognition accuracy.

Table.2.1 Classification results of MPEG-7 CE-shape-1 database using Euclidean distance

	Salt &pepper noise				
	Noise free	1%	2%	3%	4%
TKMI	100%	97.18%	95.67%	91.29%	91.01%
THMI	100%	76.89%	94.36%	91.85%	89.57%
KHMI	100%	97.19%	95.81%	92.03%	90.14%
CTMI	100%	97.58 %	96.15%	93.64%	91.47%

Table.2.2 Classification results of COILL-20 objects database using Euclidean distance

	Salt &pepper noise				
	Noise free	1%	2%	3%	4%
TKMI	96.57%	95.49%	87.65%	79.14%	74.38%
THMI	97.06%	95.25%	88.24%	78.16%	75.01%
KHMI	97.35%	95.47%	87.14%	80.56%	74.64%
CTMI	98.15%	96.24%	89.58%	81.25%	76.98%

VII. CONCLUSION

In this paper, we have proposed a fast method for the computation of a new set of Charlier-Tchebichef discrete orthogonal moments. This method is performed using the bivariate discrete orthogonal polynomials of Charlier-Tchebichef and the image slice representation. The computation of CTM using this method depends only on the number of blocks, which can significantly reduce the time computation. Furthermore, we have proposed a new set of Charlier-Tchebichef's invariant moments by two methods. The robustness to noise and the accuracy of recognition of the proposed CTMI in the classification of the object are carried out and are better than that of TKMI, THMI and KHMI. These moments have desirable image representation capability and can be useful in the field of image analysis.

REFERENCES

[1] M. K. Hu, "Visual pattern recognition by moment invariants", IRE Trans. Inform. Theory, vol. IT-8, Feb. 1962, pp. 179–187.

[2] M.R. Teague, "Image analysis via the general theory of moments", J. Opt. Soc. Amer., vol. 70 , 1980, pp.920–930.

[3] Khalid M. Hosny, Image representation using accurate orthogonal Gegenbauer moments, Pattern Recognition Letters, Volume 32, Issue 6, 15 April 2011, Pages 795-804.

[4] H. Zhang, H.Z. Shu, P. Haigron, B.S. Li, L.M. Luo, Construction of a complete set of orthogonal Fourier–Mellin moment invariants for pattern recognition applications, Image and Vision Computing, Volume 28, Issue 1, January 2010, Pp 38-44.

[5] A. Khotanzad, Y.H. Hong, "Invariant image recognition by Zernike moments", IEEE Transactions on Pattern Analysis and Machine Intelligence, vol.12, 1990, pp. 489–497.

[6] C.H. Teh, R.T. Chin, "On image analysis by the method of moments", IEEE Trans. Pattern Anal. Mach. Intell., vol.10, no.4, 1988, pp.496–513.

[7] S.X. Liao, M. Pawlak, "On image analysis by moments", IEEE Trans. Pattern Anal. Mach. Intell., vol.18, no.3, 1996, pp. 254–266.

[8] R. Mukundan, S.H. Ong, P.A. Lee, "Image analysis by Tchebichef moments", IEEE Trans. Image Process, vol. 10, no. 9, 200, pp. 1357-1364.

[9] P.T. Yap, R. Paramesran, S.H. Ong, "Image analysis by Krawtchouk moments", IEEE Transactions on Image Processing, vol.12,no. 11, 2003, pp. 1367–1377.

[10] P.T. Yap, P. Raveendran, S.H. Ong, "Image analysis using Hahn moments", IEEE Trans. Pattern Anal. Mach. Intell., vol. 29, no. 11, 2007, pp. 2057-2062.

[11] R. Mukundan, "Some computational aspects of discrete orthonormal moments", IEEE Transactions on Image Processing, vol.13, no. 8, 2004, pp. 1055–1059.

[12] H. Zhu ,"Image representation using separable two-dimensional continuous and discrete orthogonal moments", Pattern Recognition, vol. 45, no.4, 2012, pp. 1540-1558.

[13] E.D. Tsougenis, G.A. Papakostas and D.E. Koulouriotis, "Introducing the Separable Moments for Image Watermarking in a Totally Moment-Oriented Framework", Proceedings of the 18th International Conference on Digital Signal Processing (DSP'13), pp. 1-6, 1-3 July, Santorini - Greece, 2013.

[14] E.D. Tsougenis, G.A. Papakostas and D.E. Koulouriotis, "Image Watermarking via Separable Moments", Multimedia Tools and Applications, in press.

[15] S. Lewanowicz, P. Wozny, "Two-variable orthogonal polynomials of big q- Jacobi type",Journal of Computational and Applied Mathematics, vol. 233, 2010, pp. 1554-1561.

[16] L. Fernandez, T.E. Prez, M.A. Pinar, "Orthogonal polynomials in two variables as solutions of higher order partial differential equations", Journal of Approximation Theory, vol. 163, 2011, pp. 84-97.

[17] T. Koornwinder, "Two-variable analogues of the classical orthogonal polynomials", Theory and Application of Special Functions, Proceedings of the Advanced Seminar (Madison: University of Wisconsin Press), Academic Press, 1975, pp. 435–495.

[18] C.F. Dunkl, Y. Xu, "Orthogonal Polynomials of Several Variables", Encyclopedia of Mathematics and its Applications. Cambridge University Press, Cambridge, vol. 81, 2001

[19] H. Zhu, M. Liu, H. Shu, H. Zhang and L. Luo, "General form for obtaining discrete orthogonal moments", IET Image Process., Vol. 4, no. 5, October 2010, pp. 335–352.

[20] I.M. Spiliotis , B.G. Mertzios, "Real-time computation of two-dimensional moments on binary images using image block representation," IEEE Trans. Image Process., vol. 7, no. 11, 1998, pp. 1609-1615.

[21] G.A. Papakostas , E.G. Karakasis , D.E. Koulouriotis," Accurate and speedy computation of image Legendre moments for computer vision applications", Image and Vision Computing, vol. 28, no. 3, March 2010,pp. 414-423.

[22] J. Flusser, "Refined moment calculation using image block representation", Image Processing, IEEE Transactions, vol. 9, no.11 , Nov 2000, pp.1977-1978.

[23] H.Z. Shu, H. Zhang, B. J. Chen, P. Haigron, L.M. Luo, " Fast computation of Tchebichef moments for binary and gray-scale images", IEEE Transactions on Image Processing , vol. 19, no. 12, Dec. 2010, pp.3171-3180.

[24] G.A. Papakostas, E.G. Karakasis, D.E. Koulourisotis, "Efficient and accurate computation of geometric moments on gray-scale images", Pattern Recognition, vol. 41, no. 6, 2008, pp. 1895-1904.

[25] K.M. Hosny, "Exact and fast computation of geometric moments for gray level images", Appl. Math. Comput., vol. 189, 2007, pp. 1214–1222.

[26] M. Sayyouri, A. Hmimid, and H. Qjidaa, "Improving the performance of image classification by Hahn moment invariants," J. Opt. Soc. Am. A 30, 2381-2394 (2013)

[27] M. Sayyouri ,A. Hmimd , H. Qjidaa, " A fast computation of Charlier moments for binary and gray-scale images ", Information Science and Technology Colloquium (CIST) ,   Fez, Morocco, 22-24 Oct. 2012, pp.101-105.

[28] M. Sayyouri, A. Hmimd, H. Qjidaa, "A Fast Computation of Hahn Moments for Binary and Gray-Scale Images", IEEE , International Conference on Complex Systems ICCS'12, Agadir, Morocco, November 5 & 6 -2012, pp. pp.1-6.

[29] A.F. Nikiforov, S.K. Suslov, B. Uvarov, "Classical orthogonal polynomials of a discrete variable", Springer, New York, 1991.

[30] R. Koekoek, P.A.Lesky, R.F. Swarttouw, "Hypergeometric orthogonal polynomials and their q-analogues". Springer Monographs in Mathematics. Library of Congress Control Number: 2010923797, 2010.

[31] Y. Xu, "Second order difference equations and discrete orthogonal polynomials of two variables", International Mathematics Research , vol. 8, 2005, pp. 449–475.

[32] Y. Xu, "On discrete orthogonal polynomials of several variables", Advances in Applied Mathematics, vol. 33, 2004, pp. 615–663.

[33] L. Fernandez, T.E. Perez, M.A. Perez, "Second order partial differential equations for gradients of orthogonal polynomials in two variables", Journal of Computational and Applied Mathematics, vol. 199, 2007, pp. 113–121.

[34] G.A. Papakostas, E.G. Karakasis, D.E. Koulouriotis, "Novel moment invariants for improved classification performance in computer vision applications ", Pattern Recognition, vol. 43, no. 1, January 2010, pp. 58-68.

[35] R. Mukundan, K.R. Ramakrishnan, "Moment Functions in Image Analysis", World Scientific Publisher, Singapore, 1998.

[36] http://www.dabi.temple.edu/~shape/MPEG7/dataset.html.

[37] http://www.cs.columbia.edu/CAVE/software/softlib/coil-20.php

[38] K.M. Hosny, "Fast computation of accurate Gaussian–Hermite moments for image processing applications", Digital Signal Processing, vol.22, 2012, pp. 476–485.

Mhamed Sayyouri received the B.Eng. degree in electrical engineering, and the M.S. degree in engineering science from the Faculty of science, University of Sidi Mohammed Ben Abdellah, Fez, Morocco in 2002 and 2004, respectively. He is currently pursuing the Ph.D. degree in the Department of physics, University of Sidi Mohammed Ben Abdellah, Fez, Morocco. His research interest includes image processing, pattern classification, orthogonal systems, and special functions.

Abdeslam Hmimid received the B.Eng. degree in electrical engineering, with First Class Honors, and the M.S. degree in engineering science from the Faculty of science, University of Sidi Mohammed Ben Abdellah, Fez, Morocco in 2009 and 2011, respectively. He is currently pursuing the Ph.D. degree in the Department of physics, University of Sidi Mohammed Ben Abdellah, Fez, Morocco. His research interest includes image processing, pattern classification, orthogonal systems, and special functions.

 Hassan Qjidaa received the M.S. and Ph.D. degrees in electrical engineering from Nuclear Physics Institute of Lyon, in France 1984 and 1987, respectively. Since 1987, he served as a Research Scientist at Faculty of science in the University of Sidi Mohammed Ben Abdellah, Fez, Morocco. He has been a Professor with the Department of Physics. He is currently also a Director of the Information Analysis and Micro-system Teams (IAMS), and Vice Director of the electronic signal and systems laboratory (LESSI). His current research interests are in image processing, pattern recognition, data analysis, and machine intelligence.